

Nonperturbative Flow Equations with Heat-Kernel Methods at finite Temperature ^{*†}

Bernd-Jochen Schaefer [‡]

and

Hans-Jürgen Pirner [§]

Institut für Theoretische Physik
Universität Heidelberg

May 6, 2018

Abstract

We derive nonperturbative flow equations within an effective constituent quark model for two quark flavors. Heat-kernel methods are employed for a renormalization group improved effective potential. We study the evolution of the effective potential with respect to an infrared cutoff scale k at vanishing temperature. At the first stage we omit corrections coming from the anomalous dimension. This investigation is extrapolated to finite temperature, where we find a second order phase transition in the chiral limit at $T_c \approx 130$ MeV. Due to a smooth decoupling of massive modes, we can directly link the low-temperature four-dimensional theory to the three-dimensional high-temperature theory and can determine universal critical exponents.

*Talk given by the first author at Research Workshop on Deconfinement at Finite Temperature and Density, JINR Dubna, Russia, October 1-29, 1997

[†]supported by GSI, Darmstadt

[‡]e-mail address: schaefer@hybrid.tphys.uni-heidelberg.de

[§]e-mail address: pir@dxnhd1.mpi-hd.mpg.de

1 Introduction

The linear σ -model has become one of the most used working tools for the investigation of the chiral phase transition in QCD. It shares an adequate realism with good practicality in applications. Besides the study of equilibrium phenomena, the σ -model has also been widely applied to calculations of the disoriented chiral condensate. In a series of ground-breaking papers Wetterich and his group [1, 4] have applied renormalization group methods to calculate the parameters of the σ -model for all resolution scales. The fundamental idea is to follow the dynamics of the system by integrating out quantum fluctuations in infinitesimal intervals from a high momentum scale to the far infrared [2, 3]. In practice these exact renormalization group flow equations have to be truncated in a similar way to Schwinger-Dyson equations. They allow to treat the critical fluctuations of the long range σ - and $\vec{\pi}$ -fields near the second order phase transition, where mean field methods or sub summations of the effective mass type are insufficient. This approach also has to make approximations on the form of the effective action. In the following paper we follow the spirit of this renormalization group approach, parameterizing the shape of the effective potential. In fact we only allow quartic and quadratic couplings in the effective mesonic potential. This approximation together with a novel heat-kernel infrared cutoff prescription allows us to derive new and very transparent formulae for the evolution equations. Since our cutoff function is different from previous work it allows to see effects of such a variant of the cutoff functions used in Wetterichs group [1, 4]. The main aim of our contribution is to give analytical insight into the physics inherent in the method of evolution equations.

For high resolution, i.e. short distance processes fundamental QCD with quarks and gluons is the most efficient theory. A typical scale associated with perturbative QCD is $\Lambda \geq 1.5$ GeV. RHIC and LHC physics for secondary particles with $p_{\perp} \geq \Lambda$ will be dominated by such processes. In nucleus nucleus collisions, however, scattering at smaller momentum scale will be non negligible. Since the strength of the QCD interactions increases with decreasing momentum transfer, characteristic $\bar{q}q$ bound states will form and influence the dynamics at larger distances. A typical resolution where these processes start to become important is $\Lambda_{\chi SB} \approx 1.0$ GeV. Below this scale the vacuum changes and acquires a quark condensate and/or meson condensate. In a recent paper on deep inelastic scattering [5] it has been shown that a photon with varying resolution Q^2 is a good physical probe to see the transition from partons to constituent quarks experimentally. Around $Q^2 = 1$ GeV² the behavior of the structure function F_2 changes qualitatively as a function of Q^2 indicating that nature knows about the phenomenon of chiral symmetry restoration. We think that our heat-kernel cutoff restricting the virtualities of the intermediate states corresponds to the resolution scale of the photon. We use the experimental indication for the transition at 1 GeV as input to our calculation. In the spontaneously broken phase of chiral symmetry the constituent quark mass will increase with decreasing resolution and remain finite down to $\Lambda \approx \Lambda_{QCD}$. Around this scale the confining gluon configurations make themselves felt via confining forces. In the interval $\Lambda_{QCD} \leq k \leq \Lambda_{\chi SB}$ the dynamics is governed by constituent quarks inter-

acting via pions and σ -mesons. One sees nicely in our approach how the different quantum fluctuations from the σ -mesons and constituent quarks become unimportant when the infrared scale parameter becomes smaller than the respective masses of these states. These modes then decouple from the further evolution, leaving the zero mass pions alone in the evolution.

After having solved the evolution equations at zero temperature for reasonable starting values of the coupling constants, we pursue the evolution at finite temperature. Here the relevant parameter is the ratio of the temperature over the infrared scale parameter. Decoupling now sets in when the ratio of masses plus the Matsubara frequencies over the infrared scale becomes large. At high temperatures the summation over Matsubara frequencies is dominated by the lowest mode, thereby reducing the dynamics to the corresponding three-dimensional field theory, which is the purely bosonic $O(4)$ -model. We find for the critical index $\beta = 0.40$ which is in good agreement with the results from Monte Carlo calculations [8], ϵ -expansions [11] and of [4, 9].

The outline of the paper is as follows: In section 2 we derive the evolution equations assuming a fixed parameterization of the effective potential. In section 3 we give the explicit expressions of the differential equations for the broken and symmetric phase both for zero and finite temperature. Section 4 is devoted to a presentation and discussion of the results obtained after numerical integration of the evolution equations.

2 Effective action with infrared cutoff

In this section we show the derivation of the flow equation for the $SU(2) \times SU(2)$ constituent quark model (CQM).

The partition function for the $SU(2) \times SU(2)$ model at zero temperature is given by

$$Z[J = 0] = \int \mathcal{D}q \mathcal{D}\bar{q} \mathcal{D}\sigma \mathcal{D}\vec{\pi} \exp\left\{-\int d^4x (\mathcal{L}_F + \mathcal{L}_B)\right\} \quad . \quad (1)$$

We omit external sources J and investigate the chiral limit. The Euclidean space lagrangian in $d = 4$ dimensions looks like

$$\mathcal{L}_F = \bar{q}(x) (\gamma_E \partial_E + g(\sigma + i\vec{\tau}\vec{\pi}\gamma_5)) q(x) \quad , \quad (2)$$

$$\mathcal{L}_B = \frac{1}{2} \left((\partial_\mu \sigma)^2 + (\partial_\mu \vec{\pi})^2 \right) + \frac{m_0^2}{2} (\sigma^2 + \vec{\pi}^2) + \frac{\lambda_0}{4} (\sigma^2 + \vec{\pi}^2)^2 \quad . \quad (3)$$

The $T = 0$ parameters of the linear σ -model are fixed at the ultraviolet scale $\Lambda = 1.2$ GeV in a similar way as in ref. [4]. At this scale the quarks are massless partons and the σ -field has no vacuum expectation value. The mass squared $m_0^2 = (0.550 \text{ GeV})^2$ is positive reflecting a symmetric ground state. The minimum of the effective

potential $U(\sigma)$ lies at the origin. The other couplings are chosen as $\lambda_0 = 40.0$ and $g = M_q/f_\pi = 3.23$, where g is the Yukawa coupling of the constituent quarks to the mesons and its value corresponds to a constituent quark mass $M_q = 300$ MeV. We do not evolve the quark Yukawa coupling in this introductory work. The result of the evolution will be largely insensitive to the exact starting value of λ_0 . We could also have chosen $\lambda_0 = 0$ corresponding to an initial Lagrangian of the Nambu–Jona-Lasinio type without explicit mesonic interactions and non-propagating mesons [12, 13].

Integration over the fermions yields formally a non-local determinant, which can be defined by a heat-kernel representation:

$$\begin{aligned}
Z[J = 0] &= \int \mathcal{D}\sigma \mathcal{D}\vec{\pi} \det(\gamma_E \partial_E + gM(x)) \exp\left\{-\int d^4x \mathcal{L}_B\right\} \\
&= \int \mathcal{D}\sigma \mathcal{D}\vec{\pi} \exp\left\{-\frac{1}{2} \text{Tr} \log DD^+ - \int d^4x \mathcal{L}_B\right\} \\
&= \int \mathcal{D}\sigma \mathcal{D}\vec{\pi} \exp\left\{-\int d^4x \mathcal{L}_B + \right. \\
&\quad \left. \frac{1}{2} \int_{1/\Lambda^2}^{\infty} \frac{d\tau}{\tau} \int d^4x \text{tr} \langle x | e^{-\tau(-\partial_E^2 + g^2 MM^+ + g\gamma \cdot (\partial M^+))} | x \rangle \right\} \quad ,
\end{aligned} \tag{4}$$

where we use the abbreviations $M(x) = \sigma(x) + i\vec{\tau}\vec{\pi}(x)\gamma_5$ and $D = \gamma_E \partial_E + gM(x)$. We remark that the lower boundary of the integral over the proper time τ reflects the ultraviolet scale Λ which is fixed during the whole calculation. In fact, we will choose our infrared cutoff function in such a way that no ultraviolet divergences arise. Details concerning the heat-kernel representation and definitions can be found in ref. [7].

In the following we are not interested in wave function renormalizations. This means that we set the wave function renormalization constant $Z_k = 1$. We rewrite the meson fields in vectorial form with $\vec{\phi} = (\sigma, \vec{\pi})$ and $MM^+ = \vec{\phi}^2$. We omit all derivatives in the heat-kernel expression and get for the partition function

$$\begin{aligned}
Z[J = 0] &= \\
&\int \mathcal{D}\sigma \mathcal{D}\vec{\pi} \exp\left\{\frac{1}{2} \int_{1/\Lambda^2}^{\infty} \frac{d\tau}{\tau} \int d^4x \text{tr} \langle x | e^{-\tau(-\partial_E^2 + g^2 \vec{\phi}^2)} | x \rangle - \int d^4x \mathcal{L}_B\right\} \quad .
\end{aligned} \tag{5}$$

In principle, the fermion determinant is part of the functional integration over the meson fields weighted by the meson lagrangian \mathcal{L}_B . In the following, however, we will limit the integration over fermion and boson fluctuations to the one-loop level with the additional condition that the virtualities of the propagators in the loops are restricted to the interval $[k^2, \Lambda^2]$, where k^2 is the infrared and Λ^2 the ultraviolet cutoff, i.e. we do not consider the effect of modified fermions on the meson dynamics in agreement with the one-loop approximation. The total effective action governing the dynamics of the slowly varying meson fields $\vec{\phi}$ with virtualities $\leq k^2$ becomes a sum of fermionic and bosonic terms.

Using a plane wave basis for the diagonal part of the heat-kernel the effective action for the fermions Γ^F can be defined by

$$\Gamma^F(\tilde{\phi}) = \frac{1}{2} \int d^4x \int_{1/\Lambda^2}^{\infty} \frac{d\tau}{\tau} \int \frac{d^4q}{(2\pi)^4} \left\{ \text{tr}_{N_c N_f \gamma} e^{-\tau(q^2 + g^2 \tilde{\phi}^2)} \right\} . \quad (6)$$

Here the remaining trace goes over color-, flavor- and spin-space. We leave out gradients of $\tilde{\phi}$ in the exponential and restrict the background field $\tilde{\phi}$ to low virtualities. The equivalent one-loop integration over the meson fields can be done by expanding the mesonic potential $V_0 = \frac{m_0^2}{2}(\tilde{\phi}^2) + \frac{\lambda_0}{4}(\tilde{\phi}^2)^2$ around the slowly varying field configurations and one finds for the effective action for the bosons

$$\Gamma^B(\tilde{\phi}) = -\frac{1}{2} \int d^4x \int_{1/\Lambda^2}^{\infty} \frac{d\tau}{\tau} \int \frac{d^4q}{(2\pi)^4} \left\{ \text{tr}_N e^{-\tau(q^2 + \frac{\partial^2 V_0}{\partial \phi_i \partial \phi_j})} \right\} . \quad (7)$$

Here the trace goes over the (4×4) fluctuation matrices in $(\sigma, \vec{\pi})$ -space. Note the opposite sign of the bosonic and fermionic actions. The total effective action in one-loop approximation is given by the sum of both actions:

$$\Gamma(\tilde{\phi}) = \Gamma^F(\tilde{\phi}) + \Gamma^B(\tilde{\phi}). \quad (8)$$

In order to implement in this effective action the infrared cutoff on virtualities one introduces a universal k -dependent function $f_k(x = \tau k^2)$ into the proper time integrand. Note, that the proper time gives the inverse of the virtualities of the system. We mentioned this already in the discussion of the ultraviolet cutoff. The function f_k has to satisfy some general conditions: Since the action Γ_k with infrared cutoff should tend to the effective action Γ at $k = 0$, one must require that

$$f_k(0) = 1 . \quad (9)$$

To suppress modes with small virtualities the function f_k must also satisfy

$$f_k(x \rightarrow \infty) \rightarrow 0 . \quad (10)$$

This condition regularizes the infrared region of the effective action. In addition one needs a further condition on the first derivative of the cutoff function $f_k(x)$ in order to enforce that the flow equation for Γ_k is ultraviolet finite:

$$f'_k(x) = -x^2 g(x) \quad (11)$$

with $g(x)$ being a regular function in the vicinity of the origin.

One possible choice for the function $f_k(x)$ which fulfills all these requirements is

$$f_k(x) = e^{-x} \left(1 + x + \frac{1}{2} x^2 \right) . \quad (12)$$

The effective action with virtuality cutoff function $f_k(\tau k^2)$ has the following form:

$$\Gamma_k[\tilde{\phi}] = \int d^4x V_k(\tilde{\phi}) \quad (13)$$

with

$$V_k(\tilde{\phi}) = -\frac{1}{2} \int_0^\infty \frac{d\tau}{\tau} f_k(\tau k^2) \int \frac{d^4 q}{(2\pi)^4} \text{tr}_N \left\{ e^{-\tau(q^2 + \frac{\partial^2 V_0}{\partial \phi_i \partial \phi_j})} - e^{-\tau(q^2 + g^2 \tilde{\phi}^2)} \right\} . \quad (14)$$

Because of the form of $f_k(\tau k^2)$ derivatives of the effective potential with respect to k are now infrared as well as ultraviolet regularized, so a further ultraviolet cutoff Λ is no longer necessary. In the σ -model the second derivatives of the potential V_0 evaluated at $\tilde{\phi}^2$ are given by

$$\begin{aligned} \frac{\partial^2 V_0}{\partial \phi_i \partial \phi_j} &= (-\mu_0^2 + \lambda_0 \tilde{\phi}^2) \delta_{ij} + 2\lambda_0 \tilde{\phi}_i \tilde{\phi}_j , \\ &= \lambda_0 (\tilde{\phi}^2 - \phi_{k_0}^2) \delta_{ij} + 2\lambda_0 \tilde{\phi}_i \tilde{\phi}_j \end{aligned} \quad (15)$$

and the trace can explicitly be evaluated for $N = 4$ components. We find for the trace

$$\text{tr}_N e^{-\tau \frac{\partial^2 V_k}{\partial \phi_i \partial \phi_j}} = 3e^{-\tau \lambda_0 (\tilde{\phi}^2 - \phi_{k_0}^2)} + e^{-\tau \lambda_0 (3\tilde{\phi}^2 - \phi_{k_0}^2)} . \quad (16)$$

The first term on the r.h.s. of eq. (16) corresponds to the eigenvalues associated with the three pions while the other term describes the σ -meson. Since the fermionic trace is diagonal in color-, flavor- and spin-spaces we get

$$\text{tr} e^{-\tau g^2 \tilde{\phi}^2} = 4N_c N_f e^{-\tau g^2 \tilde{\phi}^2} . \quad (17)$$

Using these results we are able to calculate the derivatives of $V_k(\phi)$ which we need for the renormalization group flow equations.

3 Renormalization group flow equations

We want to study the evolution of different quantities with respect to the virtuality or momentum scale k . Since we are dealing with the possibility that the chiral symmetry is spontaneously broken we have to distinguish between two phases. For large k we start in the symmetric phase which is defined by a vanishing vacuum expectation value (VEV) ($\phi_k = 0$) of the potential. Thus by means of the derivative with respect to the fields

$$V' := \frac{\partial V}{\partial \tilde{\phi}^2} \quad (18)$$

we can define the mass m_k^2 and the coupling constant λ_k for the symmetric regime by

$$\begin{aligned} \frac{m_k^2}{2} &:= V'(\tilde{\phi}^2 = \phi_k^2 = 0) , \\ \frac{\lambda_k}{2} &:= V''(\tilde{\phi}^2 = \phi_k^2 = 0) . \end{aligned} \quad (19)$$

Taking the derivative with respect to the scale k we find the following coupled sets of flow equations for the symmetric phase ($\phi_k^2 = 0$):

$$\frac{k}{2} \frac{\partial m_k^2}{\partial k} = k \frac{\partial V'(0)}{\partial k} , \quad (20)$$

$$\frac{k}{2} \frac{\partial \lambda_k}{\partial k} = k \frac{\partial V''(0)}{\partial k} . \quad (21)$$

In the spontaneously broken region the VEV is finite ($\phi_k \neq 0$) and the mass parameter m_k^2 tends to negative values. We prefer to parameterize the evolution of the potential in this region in terms of λ_k and the minimum of the potential ϕ_k , which is defined by

$$V'(\phi_k) = 0 . \quad (22)$$

This equation enables us to find the evolution of the minimum ϕ_k . By again taking the derivative with respect to the scale k we find the flow equation for ϕ_k^2 in the broken phase ($\phi_k^2 \neq 0$). Note that we first evaluate the derivatives on the right hand sides for constant couplings with respect to k and then improve this one-loop expression by substituting the running couplings λ_k , m_k^2 and the VEV ϕ_k^2 instead of of λ_0 , m_0^2 and the VEV $\phi_{k_0}^2$. This procedure corresponds to renormalization group improvement. Thus we find the general flow equations for the broken phase

$$\frac{k}{2} \frac{\partial \phi_k^2}{\partial k} = - \frac{k}{2V''(\phi_k^2)} \frac{\partial V'(\phi_k^2)}{\partial k} = - \frac{k}{\lambda_k} \frac{\partial V'(\phi_k^2)}{\partial k} , \quad (23)$$

$$\frac{k}{2} \frac{\partial \lambda_k}{\partial k} = k \frac{\partial V''(\phi_k^2)}{\partial k} , \quad \text{if } V''' = 0 . \quad (24)$$

3.1 Evolution for $T = 0$

The heat-kernel representation of the effective potential yields the explicit evolution equations at $T = 0$. In the symmetric phase at zero temperature we use the equations (16,20,21) and get:

$$\frac{k}{2} \frac{\partial m_k^2}{\partial k} = - \frac{3\lambda_k k^2}{(4\pi)^2} \frac{1}{(1 + m_k^2/k^2)^2} + \frac{4N_c g^2 k^2}{(4\pi)^2} , \quad (25)$$

$$\frac{k}{2} \frac{\partial \lambda_k}{\partial k} = \frac{12\lambda_k^2}{(4\pi)^2} \frac{1}{(1 + m_k^2/k^2)^3} - \frac{8N_c g^4}{(4\pi)^2} . \quad (26)$$

Note the Yukawa coupling g is fixed. In general we follow the evolution equations starting at $k_0 = 1.2$ GeV with the initial values $\lambda_{k_0} = \lambda_0$ and $m_{k_0}^2 = m_0^2$. We proceed from large k to small k integrating out more and more infrared modes. Near $k = k_0$ the evolution of λ_k is dominated by the bosonic term proportional to λ_k^2 whereas the evolution of m_k^2 responds to the fermion loop. We reach chiral symmetry breaking

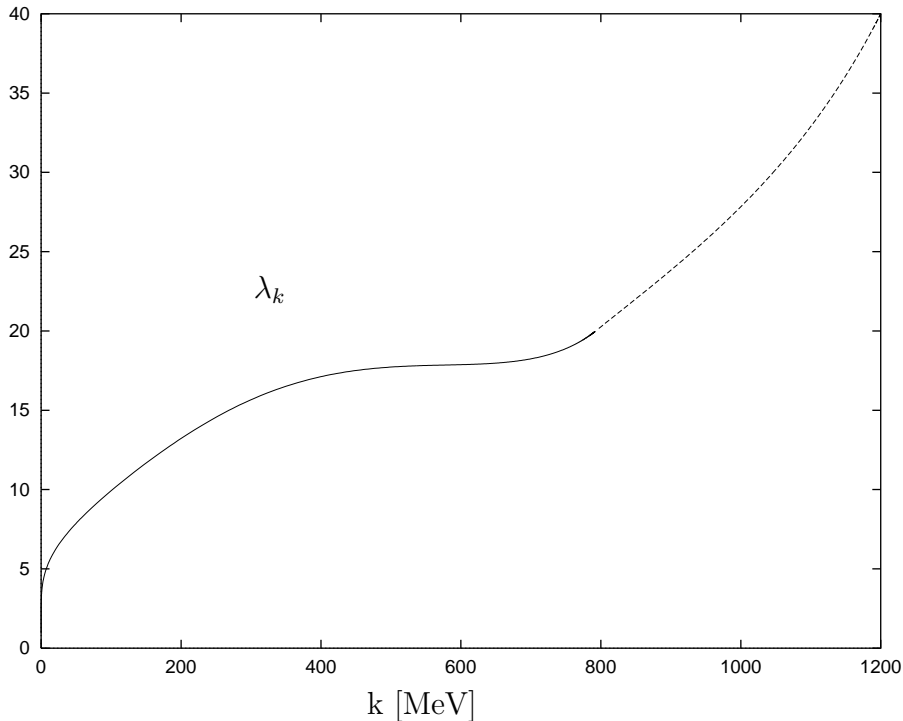


Figure 1: The evolution of λ_k with respect to the scale k .

at the scale $k = \Lambda_{\chi SB} \approx 0.8$ GeV, where we switch to the equations for the broken phase characterized by $\phi_k^2 \neq 0$.

The squared mass of the σ -meson is then given by $2\lambda_k\phi_k^2$ and the quark mass by $g\phi_k$ and the evolution equations have the following form:

$$\frac{k}{2} \frac{\partial \phi_k^2}{\partial k} = \frac{3k^2}{2(4\pi)^2} \left[1 + \frac{1}{(1 + 2\lambda_k\phi_k^2/k^2)^2} \right] - \frac{4N_c}{(4\pi)^2} \frac{k^2 g^2}{\lambda_k} \left[\frac{1}{(1 + g^2\phi_k^2/k^2)^2} \right], \quad (27)$$

$$\frac{k}{2} \frac{\partial \lambda_k}{\partial k} = \frac{3\lambda_k^2}{(4\pi)^2} \left[1 + \frac{3}{(1 + 2\lambda_k\phi_k^2/k^2)^3} \right] - \frac{8N_c}{(4\pi)^2} g^4 \left[\frac{1}{(1 + g^2\phi_k^2/k^2)^3} \right]. \quad (28)$$

The first terms on the r.h.s. of the above equations are related to the bosonic while the last parts are connected to the fermionic contributions. The factor one in the first part comes from the three pions which are massless Goldstone bosons while the second part of the bosonic term contains the contribution of the σ -meson.

The σ -meson decouples from the evolution when the term proportional to $2\lambda_k\phi_k^2/k^2$ becomes large, i.e. when the σ -meson mass over the infrared parameter k is big. (cf. [1]). The functions in squared brackets can be called threshold functions, since they describe the decoupling of the pions and σ -mesons from the evolution. With the heat-kernel method and the choice of the function $f_k(\tau)$ these threshold functions can be obtained analytically. This is an advantage of our method compared to the momentum cutoff used in refs. [1, 4]. We remark that in the heat-kernel for

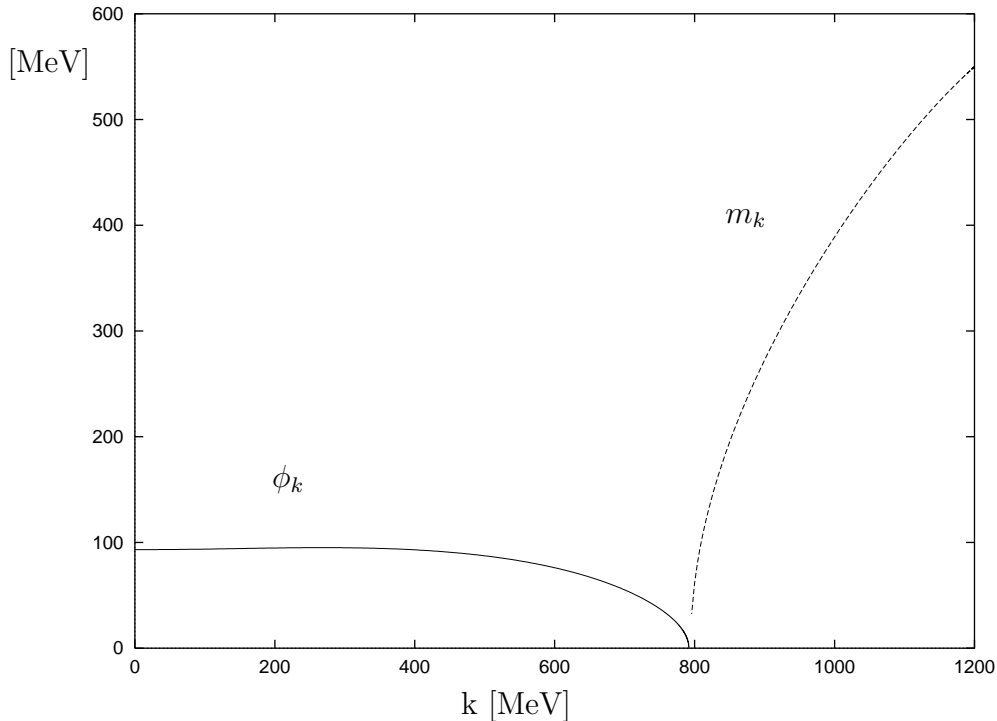


Figure 2: The evolution of the minimum of the effective potential.

the effective potential the inverse fermion propagator enters quadratically in the combination DD^+ therefore we can use the same infrared cutoff function f_k as in the bosonic integral without breaking chiral symmetry. If we want to evaluate the running coupling more care has to be used to regulate the fermion integration. One also recognizes the signs of the bosonic and fermionic contributions to the β -function. The bosons lead to an infrared stable (ultraviolet unstable) coupling, whereas the fermions counteract this tendency. Going from high k to low k one sees that the mesonic self-interaction λ_k will balance at intermediate values of k , whereas in the far infrared the boson term wins (cf. figure 1). At $k = k_{\chi SB} \approx 800$ MeV eqs.(26) and (28) become identical, also visible in figure 1 and the β -function of λ_k is continuous. The vacuum expectation value ϕ_k stabilizes at small values of k and the evolution ends with $\lim_{k \rightarrow 0} \phi_k = f_\pi$. When the heavy particles, the sigma and quarks, have decoupled, the change of the vacuum expectation value becomes proportional to k which vanishes (see figure 2). The infrared $k_{\chi SB}$ scale found in this calculation is somewhat smaller than the resolution Q of the photon found in an analysis of deep inelastic scattering [5] for the transition from the quark as a parton to the massive constituent quark. One has to wait for a more sophisticated calculation with running Yukawa coupling g_k and wave function renormalization Z_k [17] which may improve the already astonishing agreement between phenomenology and the field theoretic model.

The above equations are the evolution equations for the running of the expectation value ϕ_k^2 and quartic coupling λ_k with the infrared scale k at zero temperature.

3.2 Evolution for finite T

At finite temperature we integrate the momenta in equation (14), by splitting the zero component from the three-dimensional spatial components and convert the integration over q_0 into a summation over Matsubara frequencies $\omega_n^2 = 4\pi^2 n^2 T^2$ for the bosons and $\nu_n^2 = (2n+1)^2 \pi^2 T^2$ for the quarks.

In the symmetric phase the corresponding equations are written in terms of the positive mass parameter m_k^2 and λ_k :

$$\begin{aligned} \frac{k}{2} \frac{\partial m_k^2}{\partial k} &= -\frac{3\lambda_k^T}{(4\pi)^2} k^2 \left[\frac{3\pi T}{2k} \sum_{n=-\infty}^{\infty} \frac{1}{(1 + (\omega_n^2 + m_k^2)/k^2)^{5/2}} \right] \\ &\quad + \frac{4N_c g^2}{(4\pi)^2} k^2 \left[\frac{3\pi T}{2k} \sum_{n=-\infty}^{\infty} \frac{1}{(1 + \nu_n^2/k^2)^{5/2}} \right] , \end{aligned} \quad (29)$$

$$\begin{aligned} \frac{k}{2} \frac{\partial \lambda_k^T}{\partial k} &= \frac{12(\lambda_k^T)^2}{(4\pi)^2} \left[\frac{15\pi T}{8k} \sum_{n=-\infty}^{\infty} \frac{1}{(1 + (\omega_n^2 + m_k^2)/k^2)^{7/2}} \right] \\ &\quad - \frac{8N_c g^4}{(4\pi)^2} \left[\frac{15\pi T}{8k} \sum_{n=-\infty}^{\infty} \frac{1}{(1 + \nu_n^2/k^2)^{7/2}} \right] . \end{aligned} \quad (30)$$

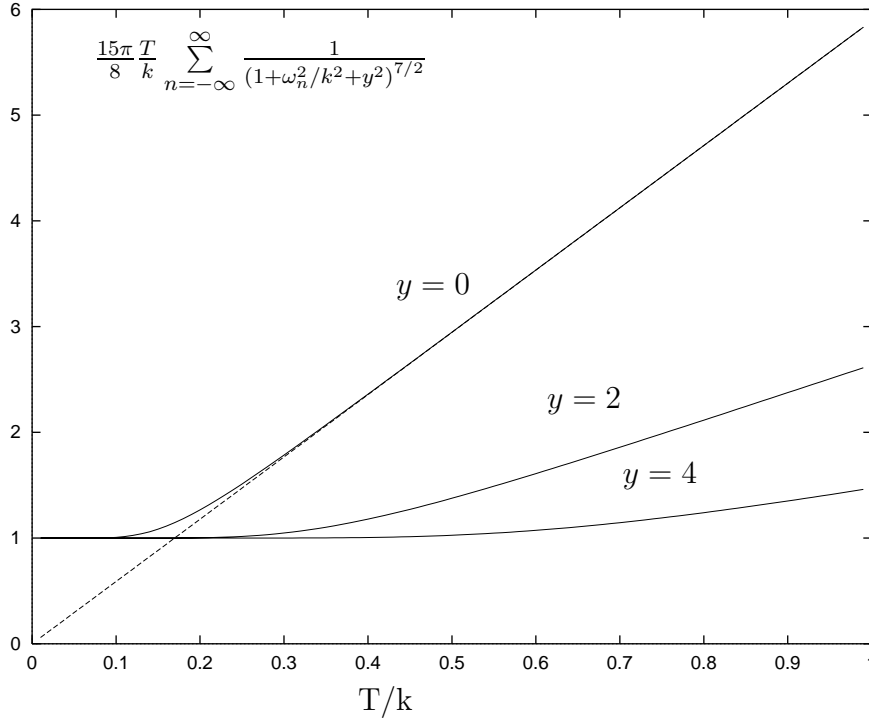


Figure 3: The bosonic threshold functions for different mass parameters $y = 0, 2, 4$ as function of T/k . The dashed line is the function $15\pi/8 \cdot T/k$ which demonstrate the linear behavior of the threshold function for large T/k .

In the broken phase one finds:

$$\begin{aligned} \frac{k}{2} \frac{\partial(\phi_k^T)^2}{\partial k} &= \frac{3k^2}{2(4\pi)^2} \left[\frac{3\pi T}{2k} \sum_{n=-\infty}^{\infty} \left\{ \frac{1}{(1 + \omega_n^2/k^2)^{5/2}} + \frac{1}{(1 + (\omega_n^2 + 2\lambda_k^T(\phi_k^T)^2)/k^2)^{5/2}} \right\} \right] \\ &\quad - \frac{4N_c}{(4\pi)^2} \frac{g^2 k^2}{\lambda_k^T} \left[\frac{3\pi T}{2k} \sum_{n=-\infty}^{\infty} \frac{1}{(1 + (\nu_n^2 + g^2(\phi_k^T)^2)/k^2)^{5/2}} \right], \end{aligned} \quad (31)$$

$$\begin{aligned} \frac{k}{2} \frac{\partial \lambda_k^T}{\partial k} &= \frac{3(\lambda_k^T)^2}{(4\pi)^2} \left[\frac{15\pi T}{8k} \sum_{n=-\infty}^{\infty} \left\{ \frac{1}{(1 + \omega_n^2/k^2)^{7/2}} + \frac{3}{(1 + (\omega_n^2 + 2\lambda_k^T(\phi_k^T)^2)/k^2)^{7/2}} \right\} \right] \\ &\quad - \frac{8N_c}{(4\pi)^2} g^4 \left[\frac{15\pi T}{8k} \sum_{n=-\infty}^{\infty} \frac{1}{(1 + (\nu_n^2 + g^2(\phi_k^T)^2)/k^2)^{7/2}} \right]. \end{aligned} \quad (32)$$

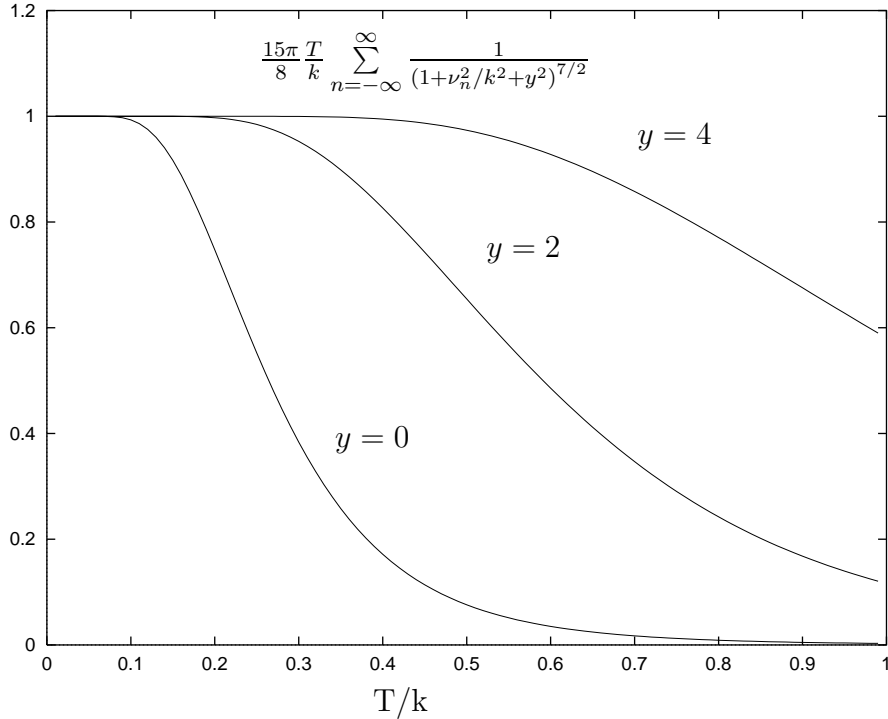


Figure 4: The fermionic threshold functions for different mass parameters $y = 0, 2, 4$ as function of T/k .

One sees that the form of the equations is unchanged concerning the dependence on the coupling constants. Only the threshold functions given in square brackets are different at finite temperature. Due to the three dimensional momentum integrations fractional powers arise in the threshold functions.

In the limit of low temperatures $T/k \rightarrow 0$ we regain our old expressions at $T = 0$, i.e. we find the relations:

$$\frac{3\pi T}{2k} \sum_{n=-\infty}^{\infty} \frac{1}{\left(1 + \left\{\frac{\omega_n^2}{\nu_n^2}\right\}/k^2 + y^2\right)^{5/2}} \rightarrow \frac{1}{(1+y^2)^2} \quad (33)$$

and also for the other threshold functions

$$\frac{15\pi T}{8k} \sum_{n=-\infty}^{\infty} \frac{1}{\left(1 + \left\{\frac{\omega_n^2}{\nu_n^2}\right\}/k^2 + y^2\right)^{7/2}} \rightarrow \frac{1}{(1+y^2)^3} \quad . \quad (34)$$

These equations guarantee the right matching of the finite temperature equations to the zero temperature equations, i.e. in the limit $T \rightarrow 0$ the set of equations for finite and zero temperature become identical. For large ratios T/k the bosonic threshold functions, given in the square brackets of eqs. (29)-(32), increase linearly in T/k . (cf. figure 3).

This increase is due to the $n = 0$ Matsubara mode in the frequency sum. In the large temperature limit the $(3 + 1)$ -dimensional system reduces to a 3-dimensional system. We plot in figure 3 the threshold functions for the bosons and in figure 4 the threshold functions for the fermions. The dimensional reduction can also be seen in the critical behavior, as will be shown in the next section. The fermionic threshold functions decrease with T/k and run to zero. There also exists a stable plateau in the vicinity of the origin for the Fermi-case as in the ref. [4].

4 Numerical results and discussion

The procedure to obtain finite temperature results is now the following. For each fixed temperature T we solve the evolution equations as functions of k with the same starting parameters as the $T = 0$ theory. The underlying idea is that at the large ultraviolet scale the finite temperature does not modify the effective theory, since the finite temperature only modifies the boundary in the imaginary time direction.

λ_{k_0}	m_{k_0} [MeV]	$k_{\chi SB}$ [MeV]	$f_{\pi}^{T=0}$ [MeV]	T_c [MeV]
30	600	787	94	$\simeq 132 \pm 1$
40	550	790	93	$\simeq 131.5 \pm 0.1$
60	450	803	93	$\simeq 133 \pm 1$
90	300	815	93	$\simeq 133 \pm 1$
120	70	823	93	$\simeq 134 \pm 1$

Table 1: Different initial values compared with the corresponding critical temperatures.

At the initial cutoff scale the momenta at the ultraviolet cutoff are anyhow so large that the theory is not affected by temperatures $2\pi T < 1.2$ GeV. Of course,

for higher temperatures also the input would have to be modified. With increasing temperature the mass parameter m_k decreases slightly more slowly towards the condensation point (cf. figure 5), but the main effect of the finite temperature occurs below $k \simeq 800$ MeV.

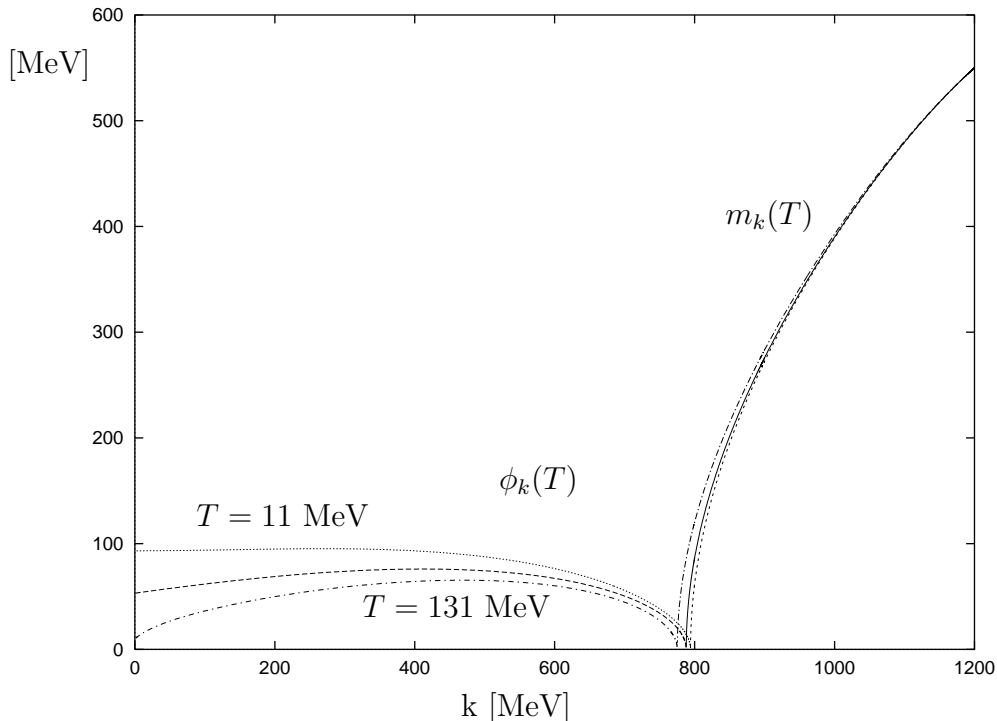


Figure 5: VEV ϕ_k and mass m_k as function of k for different temperatures. (Upper line $T = 11$ MeV, middle line $T = 111$ MeV and bottom line $T = 131$ MeV).

The threshold functions contain an additional damping due to the Matsubara frequency. Below the condensation point the boson condensate ϕ_k^2 reaches less high values at finite temperatures than before at $T = 0$. For all temperatures it decreases again with $k \rightarrow 0$, which is due to the pion loop. After optimizing the Runge-Kutta code a critical temperature

$$T_c \approx 131,5 \text{ MeV} \quad (35)$$

was found.

This temperature would be compatible with that of the Wetterich group if $f_\pi = 93$ MeV had been used in [4] even in the chiral limit [10]. They obtained a critical temperature $T_c \approx 100$ MeV by using non-analytic threshold functions and wave function and coupling constant renormalization. Both approaches share the linear sigma model with free quarks even at low temperature. In table 1 other possible initial values for λ_{k_0} and m_{k_0} at the ultraviolet scale are shown which would give the same f_π value for vanishing temperature. The corresponding critical temperature and $k_{\chi SB}$ scale are almost constant and are correlated like

$$2\pi T_c \approx k_{\chi SB} \quad . \quad (36)$$

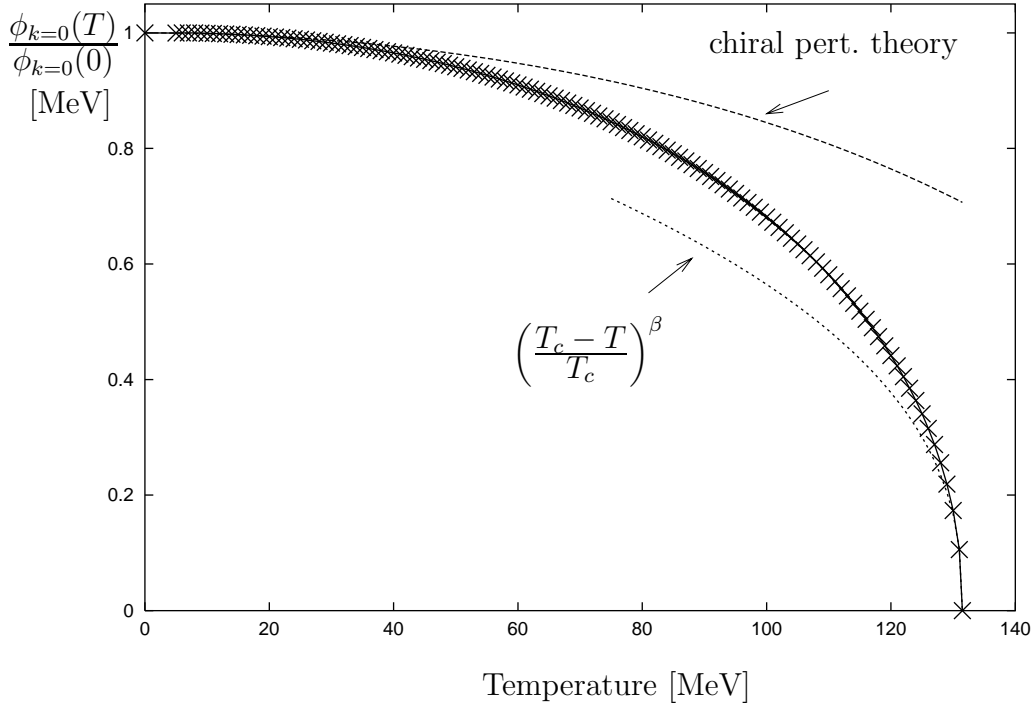


Figure 6: The order parameter as function of T .

In figure 6 we show the normalized order parameter $\phi_{k=0}(T)/\phi_{k=0}(0)$ as a function of temperature. It follows the result of chiral perturbation theory until $T \approx 35$ MeV, then it deviates because of the stronger effects of the quark loops. In chiral perturbation theory the temperature dependence of the light quark condensate for massless quarks, which is plotted in figure 6, is given by the expression

$$\frac{\langle \bar{q}q \rangle_T}{\langle \bar{q}q \rangle_0} = 1 - \frac{T^2}{8f_\pi^2} - \frac{T^4}{384f_\pi^4} - \frac{T^6}{288f_\pi^6} \ln \frac{\Lambda_q}{T} + \mathcal{O}(T^8) \quad (37)$$

with $\Lambda_q = 470 \pm 110$ MeV [15]. The purely mesonic description of the phase transition with a finite number of mesons becomes inadequate since more and more mesons become important. In the vicinity of T_c we also extrapolated in figure 6 the scaling behavior of the order parameter with our critical exponent $\beta \approx 0.40$. Still in a model without confinement of quarks the fermion loop may be overestimated cf. [16]. The renormalization group allows to include the long range correlations properly near the critical point. In fact it is possible to see scale invariance by analyzing the power law behavior of the order parameter near T_c . We plot $\log(\phi_k)$ versus $\log(T_c - T)$ in figure 7. The data points lie on a linear curve given by

$$0.40 \log(T_c - T) + (1 - 0.40) \log(T_c) - 0.30 \quad . \quad (38)$$

This yields a critical exponent $\beta \approx 0.40$ which is in good agreement with lattice results for the $O(4)$ -theory in three dimensions [8]. So in spite of the finite temperature the limit $T/k \rightarrow \infty$ enforces the dimensional reduction. One knows, that the linear sigma model lies in the same universality class as the $O(4)$ -theory, since the

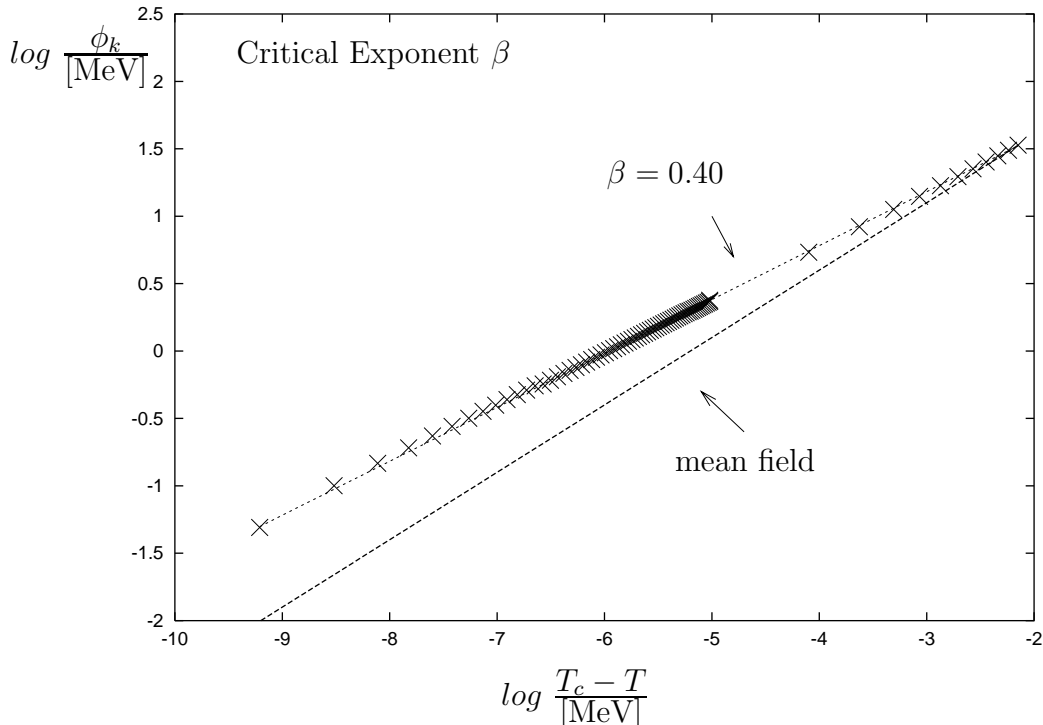


Figure 7: The critical exponent β .

fermions are not contributing to the critical fluctuations near T_c [14]. To compare the result with the mean field value $\beta = 0.5$ we also plotted this slope in the figure 7. Further investigations must study how far away from the critical point the renormalization group improvement is important for the behavior of the order parameter. An especially interesting point is to find the window for the critical dynamics. In the superconducting phase transition only the mean field behavior is experimentally relevant. From the figure 6 it seems that in chiral QCD the critical behavior influences a wider range of temperatures. In real QCD, however, the finite quark masses spoil the second order phase transition. Also gluon effects will change the behavior of the pressure in comparison with the effective linear σ -model. Numerical simulations of lattice QCD still show an inconclusive critical behavior of the order parameter. In lattice QCD the main problem is the treatment of light particles leading to large correlation lengths which are larger than the lattice size.

The presented method of heat-kernel regularization opens the way for more refined calculations also including coupling constant and wave function renormalization. Here the more delicate problem of introducing a cutoff which does not violate chiral symmetry has to be dealt with. Besides comparing the $T = 0$ theory to the behavior of deep inelastic scattering we plan to investigate the spectrum of the Dirac operator [17]. Since our method is a multi-scale analysis of the effective theory we think that the Dirac eigenmodes up to $k = 1.2$ GeV can be checked and compared to lattice calculations. Random matrix theory has been extremely successful to predict the smallest eigenvalues and correlations of nearest neighbor levels. Our method should give the broad behavior of the Dirac spectrum at $T = 0$ and for finite

temperatures. In our method the real dynamics of QCD at low resolution seems to be captured quite well. So we are optimistic about further prospects. These include the discussion of three flavor dynamics and finite quark mass effects [18]. Due to the simplicity of our cutoff function we expect also a considerable simplification in the set up and solution of three flavor dynamics. For nuclear physicist remains the ever challenging field of finite baryon density where analytical methods like our renormalization group equations are very promising to model the transition of the nuclear many body system to the quark many body system.

Acknowledgment

B.-J. S. would like to thank the organizers of the workshop, in particular D. Blaschke, for the invitation and warm hospitality. We (B.-J. S. and H.J.P.) also thank C. Wetterich and D.-U. Jungnickel for many fruitful and helpful discussions.

References

- [1] C. Wetterich, Phys. Lett. **B301** (1993) 90; C. Wetterich and N. Tetradis, Int. J. Mod. Phys. **A9** (1994) 4029.
- [2] K. G. Wilson, Phys. Rev. **B4** (1971) 3174; K. G. Wilson and I. G. Kogut, Phys. Rep. **12** (1974) 75; F. Wegner and A. Houghton, Phys. Rev. **A8** (1973) 401; F. Wegner in *Phase Transitions and Critical Phenomena*, vol. 6, eds. C. Domb and M.S. Greene, Academic Press (1976); J.F. Nicoll and T.S. Chang, Phys. Lett. **62A** (1977) 287; S. Weinberg in *Critical Phenomena for Field Theorists*, Erice Subnucl. Phys. (1976) 1;
- [3] J. Polchinski, Nucl. Phys. **B231** (1984) 269;
- [4] D.-U. Jungnickel and C. Wetterich, Phys. Rev. **D53** (1996) 5142, hep-ph/9505267; J. Berges, D.-U. Jungnickel and C. Wetterich, *Two Flavor Chiral Phase Transition from Nonperturbative Flow Equations*(1997), hep-ph/9705474.
- [5] H. G. Dosch, T. Gousset and H. J. Pirner, *Nonperturbative γp^* Interaction in the Diffractive regime*, to be published in Phys. Rev. D (1997), hep-ph/9707264.
- [6] R. Floreanini and R. Percacci, Phys. Lett. **B356** (1995) 205.
- [7] B.-J. Schaefer and H. J. Pirner, *Application of the heat-kernel method at finite temperature*, to be published in Nucl. Phys. A (1997), hep-ph/9706258.
- [8] K. Kanaya and S. Kaya, Phys. Rev. **D51** (1995) 2404.

- [9] T.R. Morris and M.D. Turner, [hep-th/9704202](#).
- [10] J. Berges and D.-U. Jungnickel, private communication.
- [11] G. Baker, D. Meiron and B. Nickel, *Phys. Rev.* **B17** (1978) 1365.
- [12] T. Eguchi, *Phys. Rev.* **D14** (1976) 2755; S. P. Klevansky, *Rev. Mod. Phys.* **64** (1992) 649.
- [13] D. Ebert, Th. Feldmann and H. Reinhardt, *Phys. Lett.* **B388** (1996) 154; D. Ebert and H. Reinhardt, *Nucl. Phys.* **A271** (1986) 188.
- [14] R. D. Pisarski and F. Wilczek, *Phys. Rev.* **D29** (1984) 338.
- [15] J. Gasser and H. Leutwyler, *Phys. Lett.* **B184** (1987) 83; P. Gerber and H. Leutwyler, *Nucl. Phys.* **B321** (1989) 387; D. Toublan, *Pion Dynamics at Finite Temperature*, [hep-ph/9706273](#).
- [16] H. J. Pirner and M. Wachs, *Nucl. Phys.* **A617** (1997) 395.
- [17] G. Papp, H. J. Pirner and B.-J. Schaefer, work in progress.
- [18] Z. Aouissat, B.-J. Schaefer and J. Wambach, work in progress.